Bioconjugate Chemistry

Editors' Choice

pubs.acs.org/bc

Article

A FAM-Binding Bispecific Antibody for Productive Delivery of siRNA to Skin by Light-Activatable Silencing

Ruolin Xu and Wanyi Tai*

Cite This: https://doi.org/10.1021/acs.bioconjchem.6c00308

Read Online

ACCESS | Metrics & More | Article Recommendations | Supporting Information

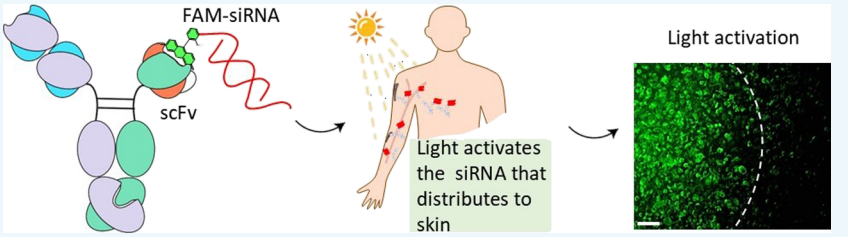

ABSTRACT: Small interfering RNA (siRNA) achieves significant clinical success in treating liver-related diseases. However, its broader application remains constrained by the low productiveness of extrahepatic delivery owing to the endosomal escape bottleneck. Here, we reported a fluorescein (FAM)-binding bispecific antibody (Fab-scFv-Fc bsAb) that can recruit one molecule of FAM-labeled siRNA and deliver productively to skin tissues by light-activatable silencing. Resembling the canonical antibody−siRNA conjugate, bsAb forms a stable monodisperse scaffold with siRNA and enables specific delivery to cells that express the corresponding antigen. Upon light radiation, the FAM dye acts as a photosensitizer and promotes the cytosolic release of siRNA from endosomes, which enhances the silencing activity > 10 times stronger than the control without photostimulation. Over 90% of target mRNA expression could be knocked down after irradiation by light with intensity comparable to the midday sunlight (100 k lux) for 5 min. In vivo, bsAb extends the siRNA half-life to 26 h and supports the productive delivery to the subcutaneous tumor tissue, where light is accessible for activation. With the spatiotemporal control of silencing, this antibody offers a useful siRNA delivery solution to extrahepatic skin tissues.

KEYWORDS: *Antibody−siRNA conjugate, photostimulation, light-activatable silencing, Fab-scFv-Fc, photochemical internalization, endosomal escape*

INTRODUCTION

Small interfering RNA (siRNA)-based therapeutics enable the precise modulation of disease-relevant gene expression, representing a type of revolutionary therapeutic modality.[1] As of April 2026, eight siRNA drugs have been approved by the U.S. Food and Drug Administration (FDA); however, all of them focus on the treatment of liver-related diseases. Currently, the *N*-acetylgalactosamine (GalNAc)−siRNA conjugate is the prevailing technology in siRNA drug development. The success of GalNAc technology relies on the "hot receptor" feature of the asialoglycoprotein receptor (ASGPR), which is characterized by high receptor number, rapid internalization, and fast recycling (turnover) in its endocytic pathway.[2] This feature allows GalNAc−siRNA to be massively taken up by hepatocytes via ASGPR, which eventually induces effective gene silencing in the liver even though the endosomal escape efficiency is very low (< 0.1%).[3] The subsequent study by Tsukasa Sugo in 2016 found that the transferrin receptor 1 (TfR1), also known as cluster of differentiation 71 (CD71), is another such type of "hot receptors", and antibody−siRNA conjugate (ARC) specific to TfR1 can trigger strong gene silencing without the assistance of cationic agents.[4] The discovery prompts the development of the first ARC pipeline (Delesiran, AOC 1001) entering the phase 3 clinical trial (NCT06411288), albeit failing to meet the endpoint in 2026.[5] Despite the progress of these siRNA delivery technologies, the "hot receptor" is very rare and difficult to discover, making the extrahepatic delivery largely stagnated and confined to limited tissues (muscle, heart).[6]

Scientists in the field of antibody−drug conjugates (ADCs) have identified more than 100 receptors with unique tumor/tissue specificity that can be used for drug delivery.[7,8] However, most receptors, including the famous human epidermal growth factor receptor 2 (HER2), have a slow turnover rate and low receptor abundance in cells compared to those "hot receptors".[9] Generally, siRNA delivery by these "cold receptors" is extremely low in efficiency. Here, it emphasizes particularly the copy number of siRNA traversing the endosomal barrier to elicit the RNA interference (RNAi) but not the siRNA of total uptake. To achieve an effective silencing via these "cold receptors" for

Received: June 7, 2026
Revised: October 23, 2026
Accepted: October 30, 2026

Downloaded from pubs.acs.org/bcches/article-pdf/doi/10.1021/acs.bioconjchem.6c00308/6922196/7bc6c00308.pdf by WUHAN UNIV user on 18 November 2026

© XXXX American Chemical Society

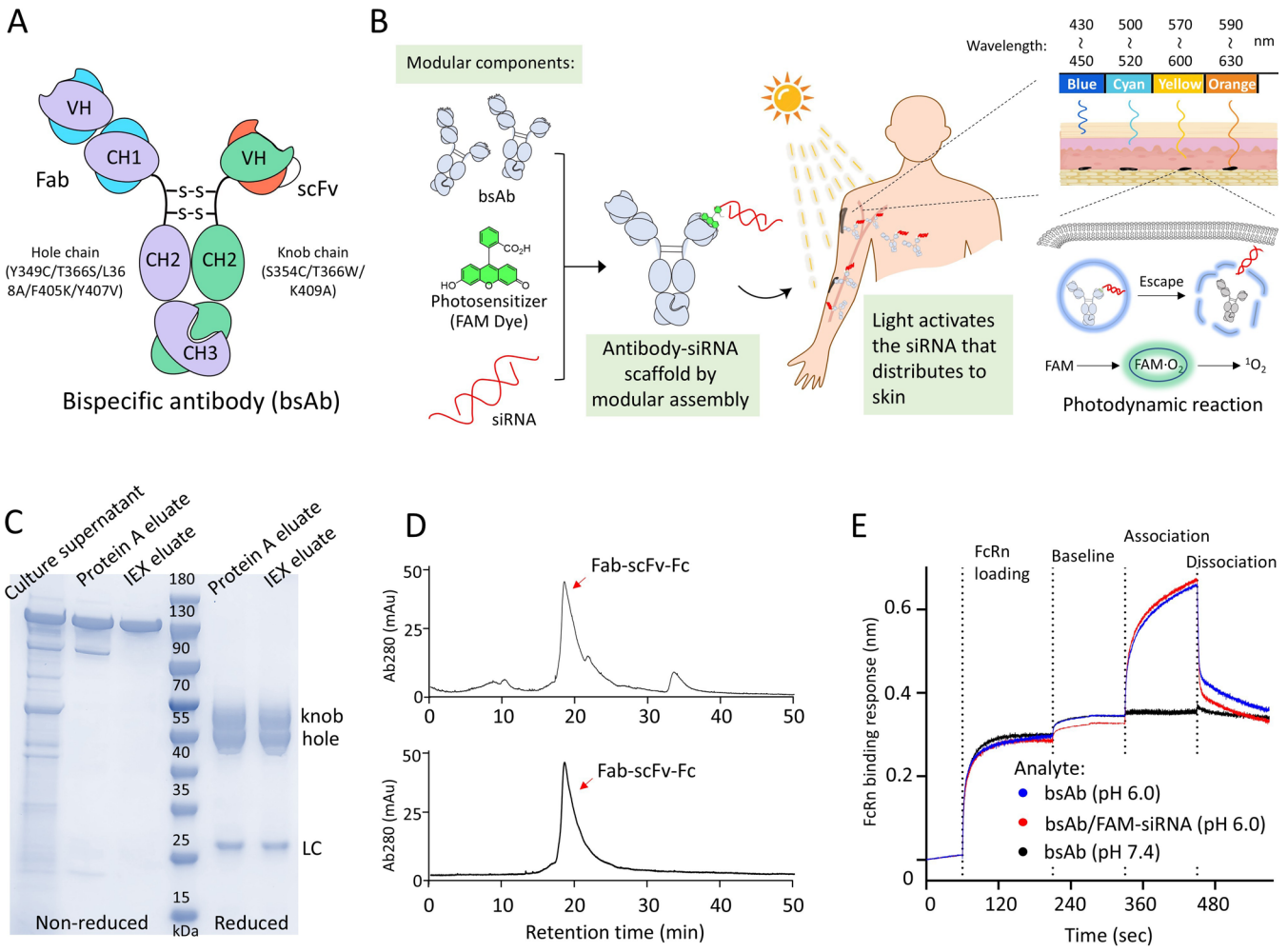

Figure 1. Generation of Fab-scFv-Fc bsAb for siRNA delivery. (A) Schematic illustration of the Fab-scFv-Fc bispecific construct. The knob and hole chains are covalently connected through two disulfide bonds in the hinge region and an engineered disulfide in the knob−hole interface (undepicted). (B) A diagraph showing the process of FAM-binding bsAb to deliver siRNA productively to skin by light-activatable silencing. (C) SDS-PAGE analysis of Fab-scFv-Fc bsAb contents (knob chain, hole chain, and light chain) in non-reduced and reduced conditions. (D) SEC traces of the protein A eluate (upper) and IEX eluate (bottom) with main bsAb peaks. (E) BLI analysis of FcRn binding to the bsAb antibody and its assembly with FAM−siRNA. The response curve of bsAb at neutral pH (7.4) is used as the negative control.

therapeutic purposes, it is essential to enhance the endosomal escape rate of siRNA for a productive delivery.[10] Several strategies, including cell-penetrating peptides, cationic liposomes, hydrophobic lipids, and others, have been proposed to overcome this central barrier.[11−13] However, most of these methods either show a low escape efficiency or lack clinical relevance (toxicity, instability, formulation problems, or others).[14,15]

One method that shows promise for overcoming this problem is to use light to facilitate the endosomal escape, termed the photochemical internalization (PCI).[16] In this strategy, photosensitizer molecules are co-delivered with siRNA and accumulated in the endosomal compartment. The light activation of photosensitizers triggers the production of reactive oxygen species ($^1O_2$) and then the rupture of endocytic vesicles, leading to the release of siRNA into the cytoplasmic matrix.[17] PCI is considered a minimally invasive technology that can facilitate the cytosolic delivery of many therapeutic molecules including not only siRNA.[18] Its mechanism and application, including some investigations in clinical trials,[19] have been extensively reviewed elsewhere.[20] It is worth noting that PCI, albeit a unique intervention, is currently subject to the treatment of only skin diseases, owing to the depth limit of light in tissue penetration.

In this study, we harvested the advantage of PCI technology in endosomal escape and designed a photo-responsive antibody−siRNA scaffold for productive delivery to skin tissues. The most striking benefit of our approach is the modular delivery concept that avoids the time-consuming antibody−siRNA conjugation step by using the FAM (fluorescein) dye molecule as the joint for scaffold assembly and also the photosensitizer for PCI. The scaffold design involves a bispecific antibody (bsAb), with one arm targeting cells of interest and the other arm recruiting the FAM-labeled siRNA for antibody−siRNA assembly. We demonstrated that this bsAb can productively deliver siRNA to the target cells through the "cold receptor" in vitro and in vivo when assisted by light stimulation. Its silencing effect is tunable by the intensity of light irradiation and depth of tissues, which therefore enables it to be a robust platform for gene regulation in the skin.

Downloaded from pubs.acs.org/bcches/article-pdf/doi/10.1021/acs.bioconjchem.6c00308/69221967/bc6c00308.pdf by WUHAN UNIV user on 18 November 2026

https://doi.org/10.1021/acs.bioconjchem.6c00308
Bioconjugate Chem. XXXX, XXX, XXX−XXX

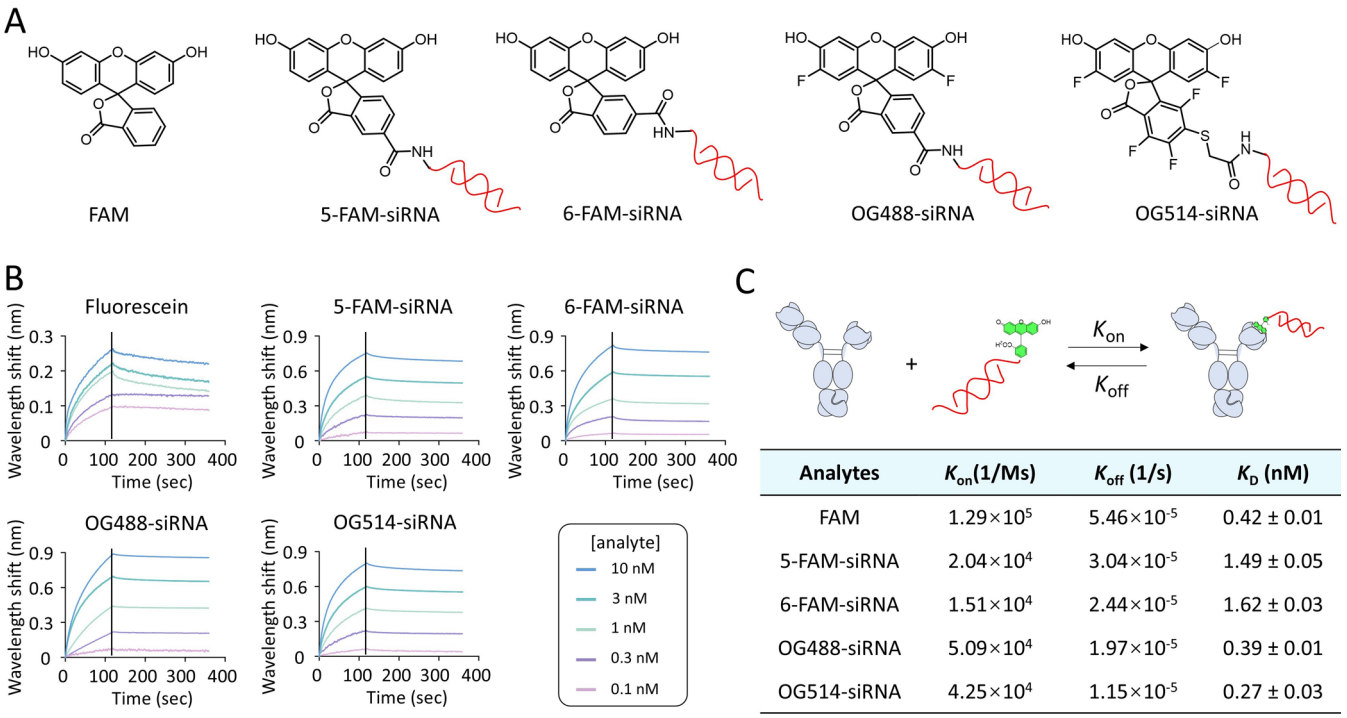

Analytes	K_{on}(1/Ms)	K_{off} (1/s)	K_D (nM)
FAM	1.29×10^{5}	5.46×10^{-5}	0.42 ± 0.01
5-FAM-siRNA	2.04×10^{4}	3.04×10^{-5}	1.49 ± 0.05
6-FAM-siRNA	1.51×10^{4}	2.44×10^{-5}	1.62 ± 0.03
OG488-siRNA	5.09×10^{4}	1.97×10^{-5}	0.39 ± 0.01
OG514-siRNA	4.25×10^{4}	1.15×10^{-5}	0.27 ± 0.03

Figure 2. Dye−siRNA conjugates and assembly with Fab-scFv-Fc. (A) Structures of FAM derivatives and their siRNA conjugates. The FAM dyes were conjugated with the aminohexyl group (amino-C6) at the 5′ end of the siRNA sense strand. (B) BLI traces showing the binding kinetics of immobilized Fab-scFv-Fc with serial dilutions of FAM and dye−siRNA conjugates. (C) Values of kinetic and affinity constants measured by BLI.

RESULTS

Fab-scFv-Fc Construct and siRNA Assembly

As a proof of concept, we developed a Fab-scFv-Fc bsAb with dual specificity against the HER2 receptor and FAM dye, respectively (Figure 1A). The Fab arm encompassing the Fab domain from Trastuzumab is fused to the IgG1 Fc domain for HER2 targeting.[21] It is engineered as the hole chain by a typical knob-into-hole (KiH) substitution (T366S, L368A, F405K, Y407V) and the Y349C mutation previously reported to add an interchain crosslink.[22] The scFv arm includes a VH-VL domain from antibody 4-4-20 to recognize the FAM dye molecule. The anti-FAM 4-4-20 is a well-known murine antibody that has been discovered and well characterized since the 1980s in academia.[23] Despite targeting the small-molecule antigen, the 4-4-20 antibody, including its fragment Fab and scFv, displays a picomolar affinity (K_D, 2.9×10^{-10} M) to FAM in the phosphate-buffered saline (PBS).[24,25] This high affinity endows a stable scFv/FAM complex that is durable in the mouse serum (Figure S1). The knob chain bearing scFv has substitutions of S354C, T366W, and K409A for heterodimerization with the hole chain.[26] It's noting that the mutations of K409A in the knob chain and F405K in the hole chain are not a classic KiH, but they could effectively inhibit Fc homodimer formation during protein expression.[27]

To obtain a monodisperse antibody−siRNA scaffold, the FAM dye molecule is covalently linked with siRNA and assembled with bsAb (Figure 1B). This scaffold resembles the prevailing ARC of DAR1 (drug-to-antibody ratio ∼ 1), but is much easier to generate.[28] Following systemic administration, the antibody−siRNA scaffold can circulate in the bloodstream and distribute throughout the body including the skin. Different from internal organs, the skin tissue is accessible by light, albeit with a penetration limit varying with wavelengths. After exposure to visible light (blue to orange), siRNAs in the skin could be activated by the photodynamic reaction and elicit a robust RNAi effect. Synergic with a skin-targeting Fab arm, the scaffold may achieve a productive delivery of siRNA to skin cells while minimizing the off-target effect. As a starting point for demonstration (demo), we chose the HER2-specific Fab (Trastuzumab) for Fab-scFv-Fc engineering. Despite the weak expression of HER2 in the skin tissue, the HER2-positive subcutaneous xenograft is accessible by light and could be a feasible model for in vivo evaluation.

Upon expression in the 293F suspension cells, the knob chain, hole chain, and light chain can assemble into the bsAb molecule Fab-scFv-Fc, but it coexists with the homodimer species and light chain-missing byproducts (Figure 1C). We first captured Fc-containing species using protein A affinity chromatography and then analyzed the eluate using analytical size-exclusion chromatography (SEC). As shown in Figure 1D (upper), the SEC chromatogram displays multiple distinct peaks. The major peak, eluting at 19 min, contains the target bsAb. Regarding other peaks, including the cubical peak at 10 min, a shoulder peak at 21 min, and a minor peak at 33 min, we were unable to isolate and characterize them experimentally owing to the small amount. However, we envisioned that they might represent aggregated species, homodimers, and antibody fragments, respectively, according to the comparative analysis of SEC chromatograms of other Fab-scFv-Fc constructs reported previously.[29−32] The protein A eluate was further purified by cation exchange chromatography (IEX) to remove byproducts. The collected eluate, with > 95% target bsAb, shows a single band at ∼ 130 kDa in the non-reduced SDS-PAGE and three distinct bands with an appropriate band-intensity ratio in the reduced condition. Biolayer interferometry (BLI) experiments showed

Downloaded from pubs.acs.org/bcches/article-pdf/doi/10.1021/acs.bioconjchem.6c00308/6922196/7bc6c00308.pdf by WUHAN UNIV user on 18 November 2026

https://doi.org/10.1021/acs.bioconjchem.6c00308
Bioconjugate Chem. XXXX, XXX, XXX−XXX

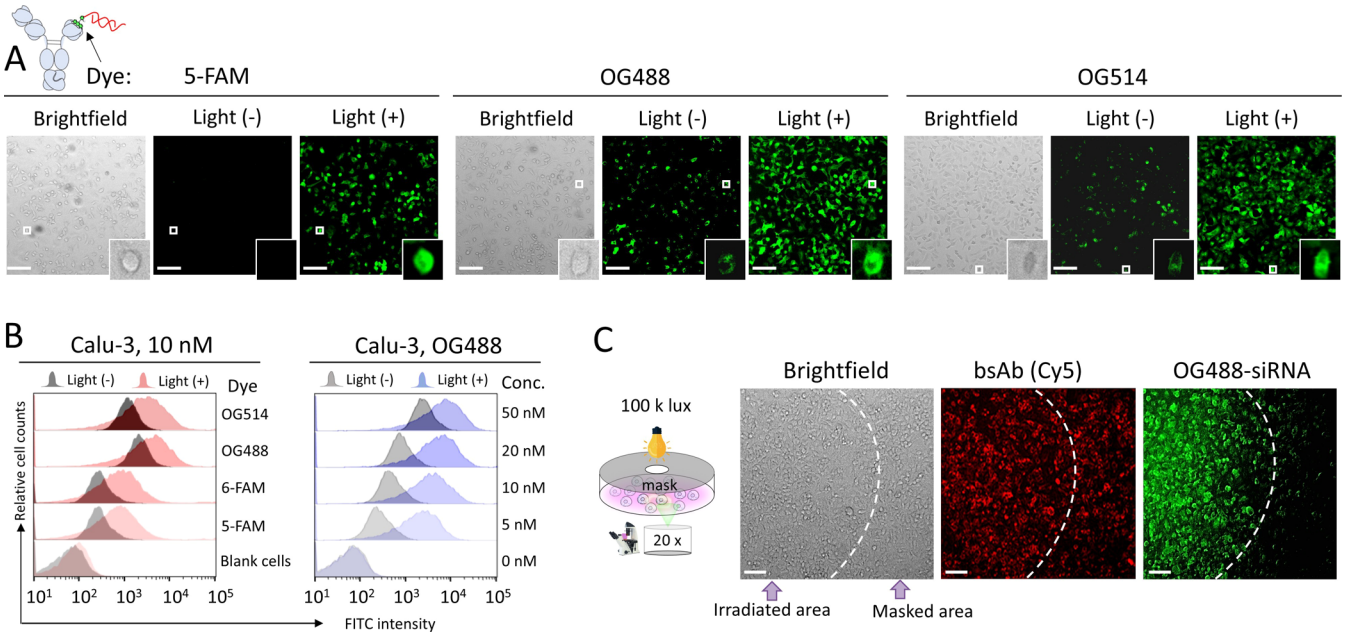

Figure 3. Light-induced endosomal escape of siRNAs labeled by 5-FAM, OG488, and OG514 dyes and delivered by Fab-scFv-Fc bsAb. (A) Fluorescent images of Calu-3 cells treated by 5-FAM−, OG488−, and OG514−based scaffolds (50 nM) for 6 h and followed by a light stimulation or no stimulation. Irradiation was performed with full-spectrum white light for 5 min. Scale bar: 80 μm. (B) The fluorescence intensity changes of the treated cells before and after light stimulation. The untreated Calu-3 cells are the blank control. (C) Region-specific photostimulation of Calu-3 cells. Calu-3 cells were incubated for 6 h with sulfo-Cy5 labeled bsAb/OG488−siRNA (50 nM), followed by 5-min irradiation with a masked white-light beam. The dashed white line indicates the boundary of the irradiated area. Scale bar: 50 μm.

that the purified bipod antibody retains its dual specificity, with dissociation constants (K_D) of 1.02 nM to HER2 ECD (extracellular domain) and 0.36 nM to FAM dye, respectively (Figure S2). Moreover, the payload FAM−siRNA, albeit rather negatively charged, has a negligible impact on FcRn binding with the Fc region of bsAb (Figures 1E and S3), indicating the retention of IgG recycling function and potential of long circulation in vivo by the bsAb/FAM−siRNA scaffold.

Selection of FAM Dyes for siRNA Docking and Photostimulation

It was reported that the endosomal escape rate after PCI has a strong correlation with the photophysical properties of dyes.[33] In spite of a high fluorescence quantum yield (ϕ), FAM's fluorescence is sensitive to the buffer pH and photobleaching. This disadvantage could be magnified in the photostimulation experiment, where the dye-bearing scaffold is entrapped in the acidic endosomes and irradiated for a long time by strong light. In order to seek a stable photosensitizer for PCI, we conjugated siRNA with four FAM derivatives (Figure 2A, and HPLC characterization available in Figure S4) and analyzed their capability to dock with bsAb for assembly. BLI analysis revealed that all four dye−siRNA conjugates exhibit high affinity with bsAb, with K_D values of 1.49 ± 0.05 nM (5-FAM−siRNA), 1.62 ± 0.03 nM (6-FAM−siRNA), 0.39 ± 0.01 nM (OG488−siRNA), and 0.27 ± 0.03 nM (OG514−siRNA), respectively (Figure 2B). It is interesting to find that all the dye−siRNA conjugates have a slower association (K_{on}) and faster dissociation (K_{off}) rates than the free FAM dye molecule in the biomolecular binding kinetics assay (Figure 2C). The observed discrepancy in kinetic measurements could be explained by the dissimilarity of the two ligands in size. Nevertheless, the conjugates with OG488 and OG514, the fluorinated derivatives of FAM, show > 4-fold higher binding affinity to bsAb than FAM−siRNA and around 2-fold better than the free FAM. It might be attributed to the increased polarity of the phenolic group and phenylcarboxylate group after inductive electron withdrawal by fluorides. The previous study with 2.7 Å structural resolution indicated that these groups in FAM have electrostatic interactions with residues of Arg-H52 (heavy chain CDRs) and Lys-L50 (light chain CDRs) in 4-4-20 antibody.[34] The fluorinated FAM dyes have a lower pK_a value and thus better fit the overall electropositive FAM-binding pocket.

It is known that pocket interaction might be accompanied by a significant increase in the dye molecular structure's rigidity, which affects the fluorescent dye's electronic state energy and enhances the photophysical properties, known as protein-induced fluorescence enhancement (PIFE).[35] However, the comparative analysis in Figure S5 revealed that the bsAb assembly has a negligible impact on the fluorescence properties of FAM dyes (the pH sensitivity and photostability). Nevertheless, OG488/OG514 dyes exhibit better fluorescent stability both in the acidic condition and after long-term photostimulation, which makes them better for the light-activatable silencing study. In the follow-up study, OG488−and OG514−siRNA conjugates were selected for scaffold assembly.

Light Activates the Endosomal Escape and Gene Silencing

Antibodies have been proven as a powerful carrier for delivering siRNA to extrahepatic tissues.[36] However, most siRNA is trapped inside the endosomal compartment, making the antibody-mediated delivery nonproductive in gene silencing.[37,38] Here, we chose the Calu-3 cell line as the model to evaluate the siRNA delivery efficiency. It has a high level of HER2 expression (Figure S6), which fits well with the delivery strategy of our engineered bsAb. We first treated cells with bsAb

Downloaded from pubs.acs.org/bcches/article-pdf/doi/10.1021/acs.bioconjchem.6c00308/69221967/bc6c00308.pdf by WUHAN UNIV user on 18 November 2026

https://doi.org/10.1021/acs.bioconjchem.6c00308
Bioconjugate Chem. XXXX, XXX, XXX−XXX

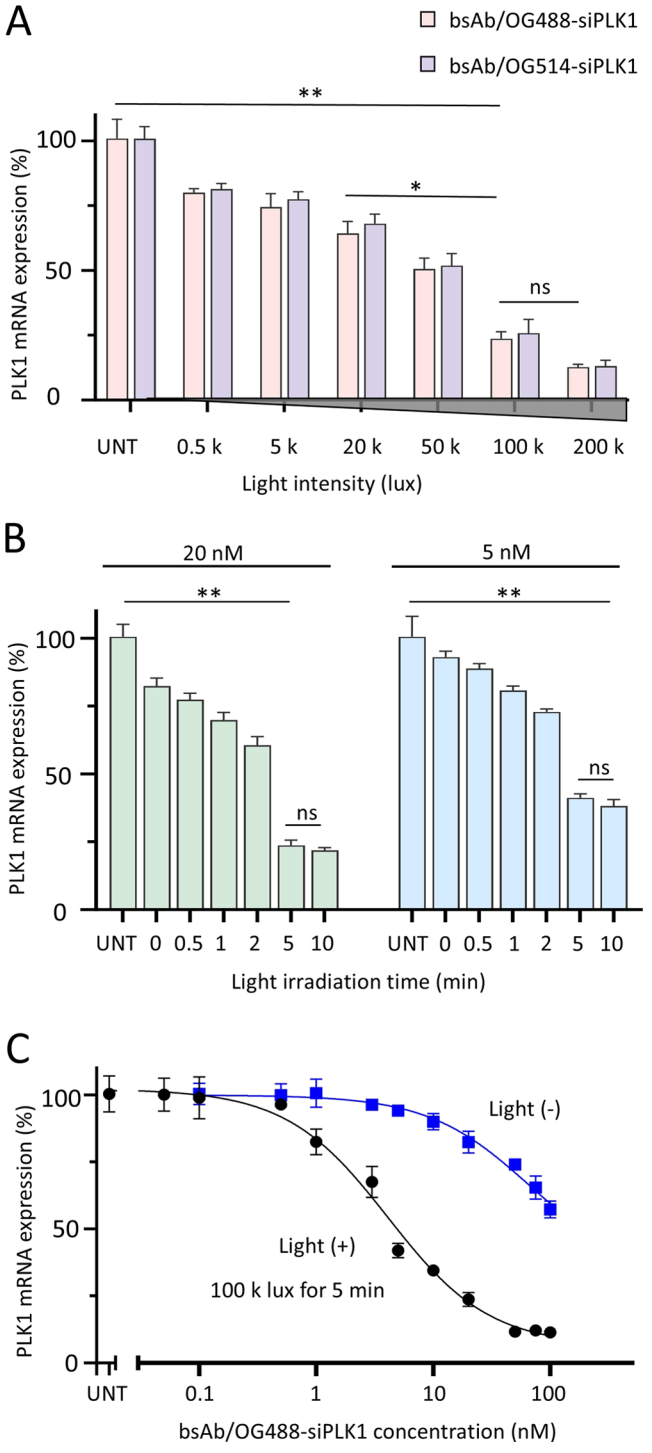

Figure 4. Light-activated gene silencing in correlation with light intensity, irradiation time, and siRNA concentration. (A) Gene silencing activity of bsAb/dye−siRNA with the varying light intensities. Cells were treated with an OG488− or OG514−based scaffold at 20 nM for 6 h, followed by 5-min irradiation with indicated light intensities. The light of 100 k lux is equivalent to the intensity of sunlight at summer midday, while 0.5 k lux is close to the moonlight intensity. Silencing efficacy was measured 24 h post-irradiation. *$P < 0.05$, **$P < 0.01$, ns, not significant. (B) The impact of light irradiation time (100 k lux) on gene silencing activity. Cells were incubated with OG488-based scaffolds of 5 nM and 20 nM, and treated as described before. *$P < 0.05$, ns, not significant.(C) Dose−response curves of gene silencing activities with or without light irradiation. Cells were treated by the same procedures above but with serial dilutions of the bsAb/OG488−siRNA scaffold. UNT, untreated control.

and traced the siRNA distribution without photostimulation. As shown in Figure 3A, the internalized siRNA, with conjugation of either FAM, OG488, or OG514 dyes, all exhibited a punctuate cytoplasmic distribution. Colocalization with the LysoTracker Red staining by the confocal imaging experiment confirmed its entrapment in the endosomal/lysosomal compartment (Figure S7). A marginal difference was observed in the FAM group, where cells emitted a relatively fainter green fluorescence than OG488−siRNA and OG514−siRNA. It could be explained by the pH effect of FAM fluorescence in the acidic endosomes. Five min after light exposure (∼ 100 k lux), we observed a remarkable redistribution of siRNA, which is evidenced by the widespread fluorescence signal throughout the cytosol. As expected, the delivery is cell-type-specific. This bsAb/dye−siRNA scaffold shows little effect in HER2-negative MDA-MB-231 cells, neither with nor without light irradiation (Figure S8), suggestive of the HER2 dependence. In Calu-3 cells treated by the FAM-based scaffold, the intensity of the dispersed fluorescence signal is weaker than in those treated by scaffolds of OG488 and OG514 dyes (Figure S9), indicating that the latter two have better PCI activity in the acidic endosomes. To better quantify the photostimulation effect, we analyzed the fluorescence intensity of cells before and after light stimulation by flow cytometry. Overlaid histograms in Figure 3B show a similar trend to the microscopic images in Figure 3A. Moreover, a clear dose-response relationship was observed, indicative of the active role of fluorescent dyes in the endosomal escape.

Figure 3C shows a region-specific control of OG488−siRNA's endosomal escape and activation by the photomask technique. The dispersed green fluorescence in the cytosol is observed only in the irradiated area. The result indicates that siRNA is released into the cytosol by the photostimulation of OG488 dyes. Upon light irradiation, endosomal membranes are thought to be destabilized by singlet oxygen ($^1O_2$) generated via the PCI.[39] This hypothesis was supported by the detection of intracellular ROS generation using the dihydroethidium (DHE) probe (Figure S10). Several groups have used the photostimulation to induce the cytosolic distribution of siRNA entrapped in the endosomes.[40−42] The Ohtsuki group could even direct the cytosolic delivery of two RNA molecules at different time points by using light sources of two wavelengths.[43]

The endosomal escape effect was further validated by measuring the light-activatable gene silencing in vitro. As shown in Figure 4A, the gene silencing effect after bsAb-mediated delivery is well correlated with the light intensity we applied for photostimulation. A significant silencing activity was observed in cells after 5 min of irradiation by a light source with a luminance over 100 k lux. It is worth noting that our white-light source covers the visible light spectrum, which is almost equivalent to the power of direct midday sunlight (∼ 100 k lux). Under this condition, the scaffold achieves over 70% mRNA silencing activity by using photosensitizer dye OG488 or OG514. Although a better activity was observed by irradiation with an even stronger light (200 k lux), it was not pursued in further study due to the potential harm to the skin. It is worth noting that no bsAb or light-induced cytotoxicity was observed even at the highest light dose we applied for the cell treatment (Figure S11). Nevertheless, we set out to screen the shortest time of photoirradiation to minimize the light exposure. As shown in Figure 4B, the RNAi activity plateaus after 5-min irradiation in groups treated by both 20 nM and 5 nM of the OG488−based scaffold, indicating that PCI activity is not accumulative by long-time stimulation. It is in agreement with the short half-life of $^1O_2$ in

Downloaded from pubs.acs.org/bcches/article-pdf/doi/10.1021/acs.bioconjchem.6c00308/6922196/7bc6c00308.pdf by WUHAN UNIV user on 18 November 2026

https://doi.org/10.1021/acs.bioconjchem.6c00308
Bioconjugate Chem. XXXX, XXX, XXX−XXX

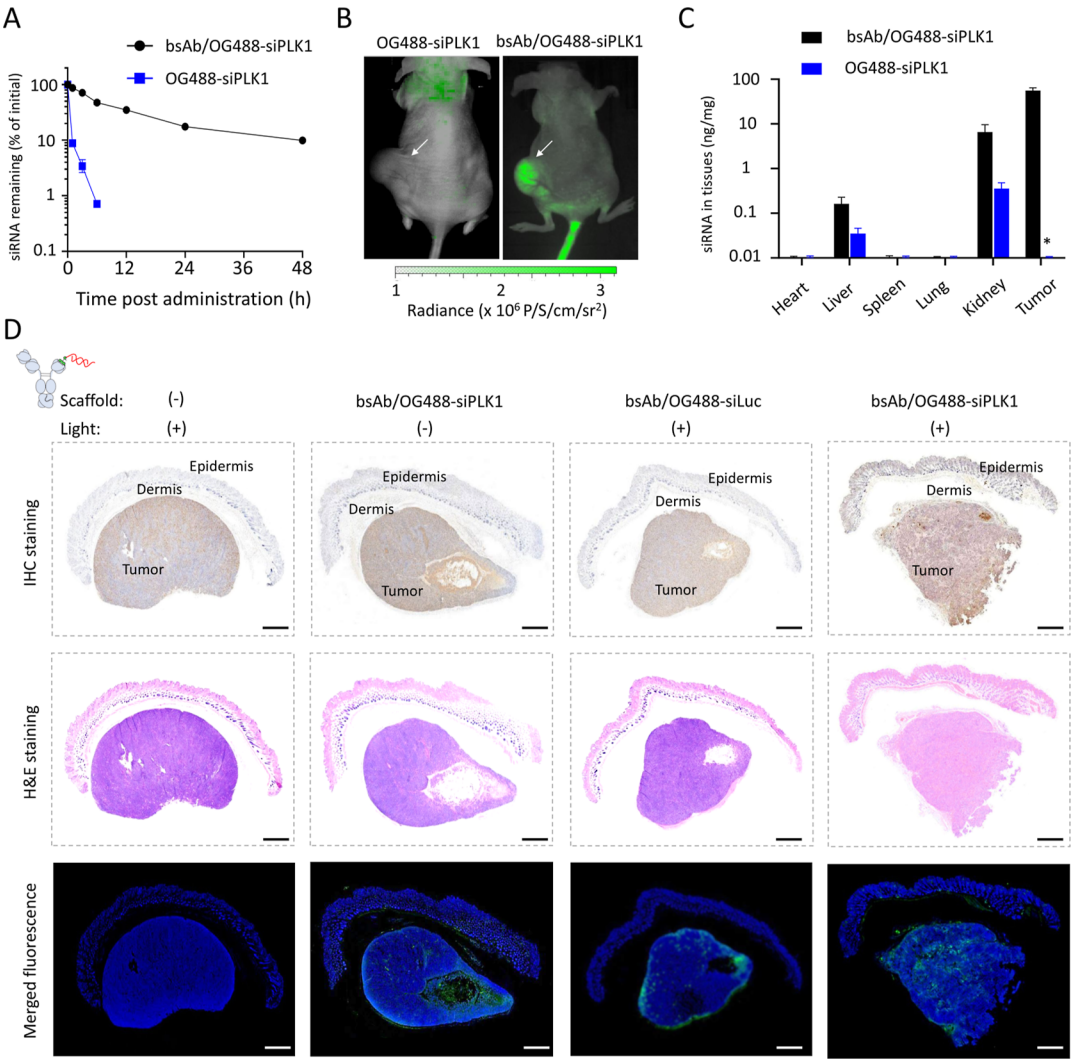

Figure 5. In vivo evaluation of siRNA delivery by FAM-binding Fab-scFv-Fc bsAb. (A) Pharmacokinetic profiles of the free OG488−siRNA and its assembly with bsAb after tail-vein injection to BALB/c mice. (B) Visualization of the OG488−siRNA deposition in the subcutaneous Calu-3 tumor 12 h after tail-vein administration. Arrows indicate the tumor sites. (C) Distribution of siRNA in the dissected tissues 12 h after tail-vein administration. *$P < 0.05$. (D) Histological analysis of skin-bearing tumor sections to reveal the correlation between light penetration and silencing activity. A light-only group, a bsAb/OG488−siPLK1 group without light irradiation, and a negative control siRNA group (bsAb/OG488−siLuc) plus light irradiation were used as controls. The brownness in the IHC staining indicates the expression level of the PLK1 protein (siPLK1's target). Green, OG488; blue, DAPI-stained nuclei. Scale bar: 1 mm.

aqueous conditions.[44] In contrast, the PCI activity is strongly correlated with the photosensitizer concentration and light intensity applied.

With the optimal condition of photostimulation, we titrated the dose−activity curve of bsAb/OG488−siRNA and compared it with the non-stimulated control. As shown in Figure 4C, the silencing activity demonstrated a clear dependence on doses in both groups. The mRNA silencing efficiency after light stimulation could achieve near-complete suppression (∼ 90%) at 75 nM, which is much more potent than the non-stimulated control group. Half-maximal silencing (EC_{50}) profiling, corresponding to a ∼ 50% mRNA reduction, revealed that the photostimulation promotes the EC_{50} at least one manifold (5 vs 100 nM). The remarkable difference in EC_{50} is in line with the hypothesis that endosomal entrapment is the rate-limiting step in ARC delivery.[45] Together, the data demonstrate that light stimulation facilitates the endosomal escape, enabling efficient cytosolic siRNA delivery and a superior silencing outcome.

Gene Silencing in Skin by Light Irradiation

Encouraged by the in vitro result, we next evaluated the potential of productive siRNA delivery in vivo after light irradiation on skin. In these animal studies, we focused particularly on the scaffold assembled by the OG488 dye because of its compatibility with the IVIS imaging system. We first analyzed the pharmacokinetics of the bsAb/OG488−siRNA scaffold in mice after the tail-vein injection. Quantitative analysis of blood siRNA concentrations by stem-loop RT-qPCR demonstrated that the scaffold siRNA exhibited a significantly prolonged systemic half-life ($t_{1/2}$ beta ∼ 26 h) compared with the free OG488−siRNA group. By 24 h, about 25% of siRNA remains associated with bsAb and present in the blood, albeit declining to ∼ 10% at 48 h. In contrast, the free siRNA group is almost nondetectable after 6 h (Figure 5A). The enhanced pharmacokinetic profile could be attributed to the IgG recycling function of bsAb and its assembly with siRNA for surpassing the renal threshold. This pharmacokinetic benefit could translate into cutaneous tissue

Downloaded from pubs.acs.org/bcches/article-pdf/doi/10.1021/acs.bioconjchem.6c00308/69221967/bc6c00308.pdf by WUHAN UNIV user on 18 November 2026

https://doi.org/10.1021/acs.bioconjchem.6c00308
Bioconjugate Chem. XXXX, XXX, XXX−XXX

targetability after systemic administration. In vivo tracing of OG488 fluorescence in mice demonstrated a strong deposition of bsAb/OG488−siRNA scaffold in the subcutaneous tumor that overexpresses HER2 receptors (Figure 5B). The subsequent study by quantifying siRNA distribution in tissues confirmed that the scaffold siRNA is most abundant in the tumor, where it is 6 times higher than that in the kidney and 100 times more than in the liver (Figure 5C). Altogether, these results demonstrate the strong tissue targetability of the bsAb/OG488−siRNA scaffold in vivo.

In order to make the siRNA in tissues productive, we irradiated the subcutaneous tumor with light (100 k lux). As the cross-section scheme shown in Figure 5D, the xenograft bolus is located in the dermis layer. Despite the weak penetrating ability, the light could pass the epidermis layer to access the tumor cells for photostimulation. Mouse epidermis generally comprises only three cell layers and is < 25 μm in thickness, whereas human epidermis commonly constitutes 6 to 10 cell layers and has a thickness between 50 and 100 μm, depending on body sites of the skin.[46] In spite of the difference in thickness, the light in visible regions generally has a penetrating depth over 1 mm,[47] which is sufficient for the subcutaneous phototherapy. As evidenced by the immunohistochemical (IHC) staining in Figure 5D, the PLK1 protein, which is targeted by the scaffold siRNA (siPLK1), is gradually downregulated following the direction of light penetration. Specifically, the quantification of DAB staining intensity revealed that the brownish pigment is lighter in the tumor region that faces the light source (Figure S12), which is in line with the proposed strategy of light-activatable silencing. In contrast, the control groups (light only, bsAb/OG488−siPLK1 without irradiation, and bsAb/OG488−siLuc with irradiation) showed little PLK1 downregulation. Meanwhile, the H&E staining in all groups shows a typical microanatomy of mouse skin and xenograft tumor without skin lesions or signs of pathology. The follow-up tracing of OG488 fluorescence (green) reveals that the siRNA is distributed broadly across the tumor tissues. Collectively, the in vivo study demonstrates that FAM-binding bsAb is an effective siRNA carrier that enables the safe, sequence-dependent, and light-activatable silencing of skin genes after systemic administration.

DISCUSSION

In this study, we developed a photosensitive bsAb scaffold (Fab-scFv-Fc) that enables targeted siRNA delivery and light-activatable gene silencing in cutaneous tissues. This system has the potential to address two major challenges impeding the extrahepatic siRNA delivery: tissue-specific targeting and limited endosomal escape. By integrating a HER2-targeting Fab domain and an anti-FAM scFv in one antibody molecule, our construct achieves both tissue specificity and non-covalent antibody/siRNA assembly without chemical conjugation. Upon light irradiation, the platform facilitates lysosomal escape via photodynamic effects, achieving up to 90% gene silencing in vitro and demonstrating effective gene knockdown of subcutaneous tissues following systemic administration.

We chose the Fab-scFv-Fc bispecific platform by leveraging its favorable properties including good stability, less mispairing chance, and smaller size.[29] It utilizes a non-covalent, high-affinity interaction between a FAM-labeled siRNA and an anti-FAM scFv, enabling a stable and stoichiometric assembly. This strategy preserves siRNA integrity and allows modular exchange of siRNA payloads without re-engineering the antibody scaffold.[48] Similar approaches have been reported by the Brinkmann group using the digoxigenin (Dig)-binding bispecific antibody.[37,49] We recently reported another bispecific antibody for siRNA delivery by using the dsRNA-binding domain (dsRBD) for noncovalent assembly of siRNAs.[26] Despite the convenience in noncovalent conjugation and siRNA payload exchange, these antibody platforms lack the endosome-disrupting ability, and the siRNA they deliver is mostly nonproductive. A key innovation of this work lies in the use of light as an external trigger to promote the endosomal escape, a rate-limiting step in the intracellular delivery of nucleic acids. While some strategies, such as CPPs or pH-sensitive polymers,[50] have demonstrated potentials, they were criticized for their limited efficiency, complex synthetic steps, and off-target toxicity.[51] Our approach leverages the photodynamic reaction of FAM derivatives, which could generate singlet oxygen to destabilize endosomal membranes. This mechanism enables spatiotemporally controlled siRNA release as evidenced by the photomask experiment. Importantly, this light-triggered escape happens without the assistance of any cationic materials, thereby minimizing the biosafety concerns associated with cationic materials.

The in vitro gene-silencing data underscore the importance of light stimulation. In the absence of light stimulation, the bsAb scaffold exhibits only weak silencing activity (approximately 50% at 100 nM). Upon light irradiation, the silencing activity is dramatically improved, reaching up to 90% gene suppression with an EC_{50} of approximately 5 nM. The light-dependent effect correlates with the PCI mechanism and the associated endosomal-disrupting activity, which is confirmed by the microscopic imaging and photomask experiment. In vivo, the Fab-scFv-Fc scaffold confers a substantially extended circulation half-life ($t_{1/2}$ beta = 26 h) compared to free siRNA, enabling sustained exposure and enhanced subcutaneous accumulation.

The bsAb platform enables the productive delivery of siRNA to skin by systemic administration. Although topical and transdermal delivery is the most popular method for administering drugs, including siRNA, to the skin,[52] systemic administration is beneficial to treat skin disease with large areas of infection or manifestation, for example, alopecia, vitiligo, rosacea, melasma, and chloasma.[53] In this proof-of-concept demo, systemic administration of the bsAb/OG488−siRNA scaffold resulted in a significant PLK1 knockdown in the subcutaneous tumor region exposed to light stimulation. This spatial selectivity highlights the spatiotemporal control afforded by light activation, which could be particularly advantageous for treating skin diseases while minimizing the off-target effect to organs deeply inside the body.

Despite the promise in the results, it is worth noting that we here utilize anti-HER2 bsAb as a model siRNA carrier. Although HER2 is a type of well-established target receptor in tumors, its expression in normal skin is limited, thus weakening the clinical relevance of this antibody to treat dermatological diseases such as psoriasis, vitiligo, cutaneous T-cell lymphoma, etc. Nevertheless, the modular nature of the Fab-scFv-Fc platform allows easy substitution of the Fab domain to adapt to other cell surface biomarkers relevant to skin diseases. Moreover, the "plug-and-play" strategy simplifies the ARC preparation procedure and also enables a rapid exchange of different siRNA payloads, which may facilitate personalized gene therapy. With further optimization of targetability, light stimulation efficiency, and photosensitizer chemistry, this platform holds promise for expanding the RNAi therapy to a wide range of skin-related diseases.

Downloaded from pubs.acs.org/bcches/article-pdf/doi/10.1021/acs.bioconjchem.6c00308/6922196/7bc6c00308.pdf by WUHAN UNIV user on 18 November 2026

https://doi.org/10.1021/acs.bioconjchem.6c00308
Bioconjugate Chem. XXXX, XXX, XXX−XXX

In sum, we successfully developed a photosensitive Fab-scFv-Fc platform to deliver siRNA productively to cutaneous tissues. Its bispecific design provides a "plug-and-play" advantage that enables the preparation of an antibody/siRNA scaffold instantly. The platform exhibits potent, dose-dependent, and light-activated gene silencing activity up to 90%, which efficiently knocks down gene expression in subcutaneous tumor tissues. While the current study focuses on HER2, the modular Fab-scFv-Fc design allows adaptation to other targets for skin diseases. In conclusion, this work provides a scalable, safe, and effective strategy for subcutaneous gene regulation, unlocking the extrahepatic potential of siRNA therapeutics.

■ ASSOCIATED CONTENT

Supporting Information

The Supporting Information is available free of charge at https://pubs.acs.org/doi/10.1021/acs.bioconjchem.6c00308.

The binding stability test in the mouse serum, BLI traces in affinity analysis, HPLC spectra, photostability test, flow cytometry analysis, confocal imaging, intracellular fluorescence intensity quantification, ROS detection, light toxicity assay, IHC staining measurement, and other information including amino acid sequences, primer sequence tables, and supplemental method details (PDF)

■ AUTHOR INFORMATION

Corresponding Author

Wanyi Tai − *Department of Pharmaceutical Engineering, School of Pharmaceutical Sciences, Wuhan University, Wuhan 430071, Hubei, China; Hubei Jiangxia Laboratory, Wuhan 430200, Hubei, China;* orcid.org/0000-0003-3589-8263; Email: wanyi-tai@whu.edu.cn

Author

Ruolin Xu − *Department of Pharmaceutical Engineering, School of Pharmaceutical Sciences, Wuhan University, Wuhan 430071, Hubei, China*

Complete contact information is available at: https://pubs.acs.org/doi/10.1021/acs.bioconjchem.6c00308

Notes

The authors declare no competing financial interest.

■ ACKNOWLEDGMENTS

This work was financially supported by the National Key R&D Program of China (Grant No. 2021YFA0909900) and the National Natural Science Foundation of China (Grant No. 82273860).

■ REFERENCES

(1) Tang, Q.; Khvorova, A. RNAi-based drug design: Considerations and future directions. *Nat. Rev. Drug Discov.* **2024**, *23* (5), 341−364.

(2) Debacker, A. J.; Voutila, J.; Catley, M.; Blakey, D.; Habib, N. Delivery of oligonucleotides to the liver with GalNAc: From research to registered therapeutic drug. *Mol. Ther.* **2020**, *28* (8), 1759−1771.

(3) Dowdy, S. F. Overcoming cellular barriers for RNA therapeutics. *Nat. Biotechnol.* **2017**, *35* (3), 222−229.

(4) Sugo, T.; Terada, M.; Oikawa, T.; Miyata, K.; Nishimura, S.; Kenjo, E.; Ogasawara-Shimizu, M.; Makita, Y.; Imaichi, S.; Murata, S.; et al. Development of antibody-siRNA conjugate targeted to cardiac and skeletal muscles. *J Control. Release* **2016**, *237*, 1−13.

(5) Malecova, B.; Burke, R. S.; Cochran, M.; Hood, M. D.; Johns, R.; Kovach, P. R.; Doppalapudi, V. R.; Erdogan, G.; Arias, J. D.; Darimont, B.; et al. Targeted tissue delivery of RNA therapeutics using antibody-oligonucleotide conjugates (AOCs). *Nucleic Acids Res.* **2023**, *51* (12), 5901−5910.

(6) Sheridan, C. Now with oligos: Antibody−oligonucleotide conjugates are the new drug modality to watch. *Nat. Biotechnol.* **2026**, *44* (1), 3−5.

(7) Maecker, H.; Jonnalagadda, V.; Bhakta, S.; Jammalamadaka, V.; Junutula, J. R. Exploration of the antibody-drug conjugate clinical landscape. *mAbs* **2023**, *15* (1), 2229101.

(8) Sasso, J. M.; Tenchov, R.; Bird, R.; Iyer, K. A.; Ralhan, K.; Rodriguez, Y.; Zhou, Q. A. The evolving landscape of antibody-drug conjugates: In depth analysis of recent research progress. *Bioconjugate Chem.* **2023**, *34* (11), 1951−2000.

(9) Springer, A. D.; Dowdy, S. F. GalNAc-siRNA, conjugates Leading the way for delivery of RNAi therapeutics. *Nucleic Acid Ther.* **2018**, *28* (3), 109−118.

(10) Cuellar, T. L.; Barnes, D.; Nelson, C.; Tanguay, J.; Yu, S. F.; Wen, X.; Scales, S. J.; Gesch, J.; Davis, D.; van Brabant Smith, A.; et al. Systematic evaluation of antibody-mediated siRNA delivery using an industrial platform of THIOMAB-siRNA conjugates. *Nucleic Acids Res.* **2015**, *43* (2), 1189−1203.

(11) Dowdy, S. F. Endosomal escape of RNA therapeutics: How do we solve this rate-limiting problem? *RNA* **2023**, *29* (4), 396−401.

(12) Pei, D.; Buyanova, M. Overcoming endosomal entrapment in drug delivery. *Bioconjugate Chem.* **2019**, *30* (2), 273−283.

(13) Mao, Q.; Quan, Y.; Chen, S.; Tai, W. Design of bifunctional RNA-binding compounds that can modulate siRNA hydrophobicity for deep penetration and gene silencing in the retina. *Mol. Ther. Nucleic Acids* **2025**, *36* (4), 102751.

(14) O'Brien Laramy, M.; Foley, D. A.; Pak, R. H.; Lewis, J. A.; McKinney, E.; Egan, P. M.; Yerabolu, R.; Dane, E.; Dirat, O.; Saunders Gorka, L.; et al. Chemistry, manufacturing and controls strategies for using novel excipients in lipid nanoparticles. *Nat. Nanotechnol.* **2025**, *20* (3), 331−344.

(15) Gould, S.; Templin, M. V. Off target toxicities and links with physicochemical properties of medicinal products, including antibiotics, oligonucleotides, lipid nanoparticles (with cationic and/or anionic charges). Data review suggests an emerging pattern. *Toxicol. Lett.* **2023**, *384*, 14−29.

(16) Selbo, P. K.; Weyergang, A.; Hogset, A.; Norum, O.-J.; Berstad, M. B.; Vikdal, M.; Berg, K. Photochemical internalization provides time- and space-controlled endolysosomal escape of therapeutic molecules. *J. Control. Release* **2010**, *148* (1), 2−12.

(17) Ohtsuki, T.; Miki, S.; Kobayashi, S.; Haraguchi, T.; Nakata, E.; Hirakawa, K.; Sumita, K.; Watanabe, K.; Okazaki, S. The molecular mechanism of photochemical internalization of cell penetrating peptide-cargo-photosensitizer conjugates. *Sci. Rep.* **2015**, *5*, 18577.

(18) Jerjes, W.; Theodossiou, T. A.; Hirschberg, H.; Hogset, A.; Weyergang, A.; Selbo, P. K.; Hamdoon, Z.; Hopper, C.; Berg, K. Photochemical internalization for intracellular drug delivery: From basic mechanisms to clinical research. *J. Clin. Med.* **2020**, *9* (2), 528.

(19) Omura, G.; Honma, Y.; Matsumoto, Y.; Shinozaki, T.; Itoyama, M.; Eguchi, K.; Sakai, T.; Yokoyama, K.; Watanabe, T.; Ohara, A.; et al. Transnasal photoimmunotherapy with cetuximabsarotalocansodium: Outcomes on the local recurrence of nasopharyngeal squamous cell carcinoma. *Auris, Nasus, Larynx* **2023**, *50* (4), 641−645.

(20) Sandland, J.; Boyle, R. W. Photosensitizer antibody-drug conjugates: Past, present, and future. *Bioconjugate Chem.* **2019**, *30* (4), 975−993.

(21) Xu, R.; Zheng, Y.; Tai, W. A single-chain fab derived drug conjugate for HER2 specific delivery. *Biomaterials* **2025**, *313*, 122798.

(22) Merchant, A. M.; Zhu, Z.; Yuan, J. Q.; Goddard, A.; Adams, C. W.; Presta, L. G.; Carter, P. An efficient route to human bispecific IgG. *Nat. Biotechnol.* **1998**, *16* (7), 677−681.

(23) Mallender, W. D.; Carrero, J.; Voss, E. W. Comparative properties of the single chain antibody andFvderivatives of mAb 4-4-20.

Downloaded from pubs.acs.org/bcches/article-pdf/doi/10.1021/acs.bioconjchem.6c00308/6922196/bc6c00308.pdf by WUHAN UNIV user on 18 November 2026

Relationship between interdomain interactions and the high affinity for fluorescein ligand. *J. Biol. Chem.* **1996**, *271* (10), 5338−5346.
(24) Herron, J. N.; Terry, A. H.; Johnston, S.; He, X. M.; Guddat, L. W.; Edmundson, A. B. High resolution structures of the 4-4-20 Fab-fluorescein complex in two solvent systems: effects of solvent on structure and antigen-binding affinity. *Biophys. J.* **1994**, *67* (6), 2167−2183.
(25) Boder, E. T.; Midelfort, K. S.; Wittrup, K. D. Directed evolution of antibody fragments with monovalent femtomolar antigen-binding affinity. *Proc. Natl. Acad. Sci. U.S.A.* **2000**, *97* (20), 10701−10705.
(26) Liu, Y.; Zheng, Y.; Xu, R.; Quan, Y.; Tai, W. Staufen dsRNA-binding domain as modules to design bifunctional antibodies for siRNA delivery. *Nucleic Acids Res.* **2026**, *54* (3), gkaf1539.
(27) Wei, H.; Cai, H.; Jin, Y.; Wang, P.; Zhang, Q.; Lin, Y.; Wang, W.; Cheng, J.; Zeng, N.; Xu, T.; et al. Structural basis of a novel heterodimericFcfor bispecific antibody production. *Oncotarget* **2017**, *8* (31), 51037−51049.
(28) Cochran, M.; Arias, D.; Burke, R.; Chu, D.; Erdogan, G.; Hood, M.; Kovach, P.; Kwon, H. W.; Chen, Y.; Moon, M.; et al. Structure-activity relationship of antibody-oligonucleotide conjugates: Evaluating bioconjugation strategies for antibody-siRNA conjugates for drug development. *J. Med. Chem.* **2024**, *67* (17), 14852−14867.
(29) Stutz, C.; Blein, S. A single mutation increases heavy-chain heterodimer assembly of bispecific antibodies by inducing structural disorder in one homodimer species. *J. Biol. Chem.* **2020**, *295* (28), 9392−9408.
(30) Nesspor, T. C.; Kinealy, K.; Mazzanti, N.; Diem, M. D.; Boye, K.; Hoffman, H.; Springer, C.; Sprenkle, J.; Powers, G.; Jiang, H.; et al. High-throughput generation of bipod (Fab × scFv) bispecific antibodies exploits differential chain expression and affinity capture. *Sci. Rep.* **2020**, *10* (1), 7557.
(31) Moore, G. L.; Bernett, M. J.; Rashid, R.; Pong, E. W.; Nguyen, D.-H. T.; Jacinto, J.; Eivazi, A.; Nisthal, A.; Diaz, J. E.; Chu, S. Y.; et al. A robust heterodimericFcplatform engineered for efficient development of bispecific antibodies of multiple formats. *Methods* **2019**, *154*, 38−50.
(32) Zhao, F.; Wu, Y.; Schaefer, K.; Zhang, Y.; Miao, K.; Yao, Z.; Ganjave, S. D.; Kumru, K.; Peters-Clarke, T. M.; Inague, A.; et al. Hijacking extracellular targeted protein degrader−drug conjugates for enhanced drug delivery. *J. Am. Chem. Soc.* **2025**, *147* (43), 39912−39925.
(33) Yarani, R.; Shiraishi, T.; Nielsen, P. E. Effective photo-enhancement of cellular activity of fluorophore-octaarginine antisense PNA conjugates correlates with singlet oxygen formation, endosomal escape and chromophore lipophilicity. *Sci. Rep.* **2018**, *8* (1), 638.
(34) Cambillau, C.; Spinelli, S.; Honegger, A.; Plückthun, A. A mutation designed to alter crystal packing permits structural analysis of a tight-binding fluorescein-scFv complex. *wwPDB* **2005**, *14* (10), 2537−2549.
(35) Hwang, H.; Myong, S. Protein induced fluorescence enhancement (PIFE) for probing protein-nucleic acid interactions. *Chem. Soc. Rev.* **2014**, *43* (4), 1221−1229.
(36) Jiao, J.; Qian, Y.; Lv, Y.; Wei, W.; Long, Y.; Guo, X.; Buerliesi, A.; Ye, J.; Han, H.; Li, J.; et al. Overcoming limitations and advancing the therapeutic potential of antibody-oligonucleotide conjugates (AOCs): Current status and future perspectives. *Pharmacol. Res.* **2024**, *209*, 107469.
(37) Schneider, B.; Grote, M.; John, M.; Haas, A.; Bramlage, B.; lckenstein, L. M.; Jahn-Hofmann, K.; Bauss, F.; Cheng, W.; Croasdale, R.; et al. Targeted siRNA delivery and mRNA knockdown mediated by bispecific digoxigenin-binding antibodies. *Mol. Ther. Nucleic Acids* **2012**, *1* (9), e46.
(38) Nanna, A. R.; Kel'in, A. V.; Theile, C.; Pierson, J. M.; Voo, Z. X.; Garg, A.; Nair, J. K.; Maier, M. A.; Fitzgerald, K.; Rader, C. Generation and validation of structurally defined antibody-siRNA conjugates. *Nucleic Acids Res.* **2020**, *48* (10), 5281−5293.
(39) Chen, W.; Deng, W.; Goldys, E. M. Light-triggerableliposomes for enhanced endolysosomal escape and gene silencing in PC12 cells. *Mol. Ther. Nucleic Acids* **2017**, *7*, 366−377.
(40) Endoh, T.; Sisido, M.; Ohtsuki, T. Cellular siRNA delivery mediated by a cell-permeant RNA-binding protein and photoinduced RNA interference. *Bioconjugate Chem.* **2008**, *19* (5), 1017−1024.
(41) Wang, X.; Xiao, X.; Feng, Y.; Li, J.; Zhang, Y. A photoresponsive antibody-siRNA conjugate for activatable immunogene therapy of cancer. *Chem. Sci.* **2022**, *13* (18), 5345−5352.
(42) Baldan, M.; Zhang, S.; Sun, Q.; Su, Y.; Mei, D.; Sun, R.; Zheng, A.; Liu, D.; Zhang, J.; Huo, R.; et al. NIR-triggered siRNAeeleaseand lysosomal escape for synergistic photothermal tumor therapy. *Int. J. Nanomedicine.* **2025**, *20*, 4863−4882.
(43) Shiraga, K.; Soe, T. H.; Matsumoto, S.; Watanabe, K.; Ohtsuki, T. Red and near-infrared light-directed cytosolic delivery of two different RNAs using photosensitive RNA carriers. *Bioconjugate Chem.* **2018**, *29* (9), 3174−3179.
(44) Murotomi, K.; Umeno, A.; Sugino, S.; Yoshida, Y. Quantitative kinetics of intracellular singlet oxygen generation using a fluorescence probe. *Sci. Rep.* **2020**, *10* (1), 10616.
(45) Liu, Y.; Quan, Y.; Mao, Q.; Xu, R.; Tai, W. Exploring the potentials of antibody−siRNA conjugates in tumor cell gene silencing without cationic assistance. *Bioconjugate Chem.* **2025**, *36* (8), 1721−1732.
(46) Salgado, G.; Ng, Y. Z.; Koh, L. F.; Goh, C. S. M.; Common, J. E. Human reconstructed skin xenografts on mice to model skin physiology. *Differentiation* **2017**, *98*, 14−24.
(47) Finlayson, L.; Barnard, I. R. M.; McMillan, L.; Ibbotson, S. H.; Brown, C. T. A.; Eadie, E.; Wood, K. Depth penetration of light into skin as a function of wavelength from 200 to 1000 nm. *Photochem. Photobiol.* **2022**, *98* (4), 974−981.
(48) Lehmann, T.; Schneider, H.; Tonillo, J.; Schanz, J.; Schwarz, D.; Hecht, S.; Anderl, J.; et al. Welding PROxAb shuttles: A modular approach for generating bispecific antibodies via site-specific protein−protein conjugation. *Bioconjugate Chem.* **2024**, *35* (6), 780−789.
(49) Metz, S.; Haas, A. K.; Daub, K.; Croasdale, R.; Stracke, J.; Lau, W.; Georges, G.; Josel, H.-P.; Dziadek, S.; Hopfner, K.-P.; et al. Bispecific digoxigenin-binding antibodies for targeted payload delivery. *Proc. Natl. Acad. Sci. U.S.A.* **2011**, *108* (20), 8194−8199.
(50) Rozema, D. B.; Lewis, D. L.; Wakefield, D. H.; Wong, S. C.; Klein, J. J.; Roesch, P. L.; Bertin, S. L.; Reppen, T. W.; Chu, Q.; Blokhin, A. V.; et al. Dynamic polyconjugates for targeted in vivo delivery of siRNA to hepatocytes. *Proc. Natl. Acad. Sci. U.S.A.* **2007**, *104* (32), 12982−12987.
(51) Chahal, G. S.; Helbig, K. J.; Parton, R. G.; Monson, E. A. The biology of endosomal escape: Strategies for enhanced delivery of therapeutics. *ACS Nano* **2026**, *20* (2), 1789−1813.
(52) Fakih, H. H.; Zain Ui Abideen, M.; Rachid, M. O.; Gross, K. Y.; Ormsby, T. J. R.; Ross, V. M.; Gagnon, R.; Dahlke, C.; Furgal, R. C.; Lochmann, C.; et al. Intradermal delivery of lipophilic siRNAs enables prolonged skin retention and sustained gene silencing in a porcine model. *Nat. Commun.* **2026**, *17* (1), 2292.
(53) Goldust, J. Systemic treatments for skin conditions: Benefits and risks of internal therapies. *Res. Clin. Dermatol.* **2024**, *7* (6), 239.

Downloaded from pubs.acs.org/bcches/article-pdf/doi/10.1021/acs.bioconjchem.6c00308/69221967/bc6c00308.pdf by WUHAN UNIV user on 18 November 2026

https://doi.org/10.1021/acs.bioconjchem.6c00308
Bioconjugate Chem. XXXX, XXX, XXX−XXX